

Thermodynamic modeling of the LiCl-KCl-LaCl₃ system with Bayesian model selection and uncertainty quantification

Rushi Gong^{1,*}, Shun-Li Shang¹, Vitaliy G. Goncharov^{2,3}, Xiaofeng Guo^{2,3}, and Zi-Kui Liu¹

¹*Department of Materials Science and Engineering, The Pennsylvania State University, University Park, PA 16802, United States*

²*Department of Chemistry, Washington State University, Pullman, Washington, 99164, United States*

³*Materials Science and Engineering Program, Washington State University, Pullman, Washington 99164, United States*

*Corresponding author

Corresponding email: rfg5281@psu.edu

Abstract

Chloride molten salts are increasingly recognized for their applications in pyroprocessing techniques for the separation of lanthanides. Understanding the thermodynamic properties of these molten salts is essential to optimize the separation process. Several thermodynamic models, including the associate model, the two-sublattice ionic model, and the modified quasichemical model with quadruplet approximation (MQMQA), are utilized to capture the complexity of molten salts. In the present work, the Bayes factor was used to guide model selection process for the thermodynamic modeling of the KCl-LaCl₃ system and provide statistical comparisons of liquid models. The results indicate that the MQMQA model is the most favorable model based on the available thermochemical data. The LiCl-KCl-LaCl₃ system was further optimized with uncertainty quantification using MQMQA. The thermodynamic properties of compounds in the KCl-LaCl₃ system were obtained from DFT-based phonon calculations. The calculated phase stability shows excellent agreement with experimental data, indicating that an appropriate model is important for accurately predicting the behavior of complex molten salts.

Keywords: Molten salts, Lanthanides, CALPHAD modeling, Bayesian model selection

Highlights:

- Thermodynamic properties at finite temperature of compounds in the KCl-LaCl₃ system obtained from DFT-based phonon calculations.
- Bayes factor for selecting thermodynamic model for the KCl-LaCl₃ liquid phase.
- Thermodynamic modeling with uncertainty quantification of the LiCl-KCl-LaCl₃ system with MQMQA for liquid phase

1 Introduction

Chloride molten salts are gaining significant attention for their potential applications in advanced nuclear reactors and pyroprocessing techniques [1–3]. Effective separation of fission products, such as lanthanides, using pyroprocessing techniques requires a comprehensive understanding of their thermodynamic properties in molten salts. The CALPHAD (CALculation of PHase Diagram) modeling [4–6] is an effective approach for investigating phase equilibrium and thermodynamic properties in multicomponent systems. For modeling of complex molten salts, various thermodynamic models within the CALPHAD framework have been developed to capture intricate behavior such as short-range ordering. These models include associate model [7], two-sublattice ionic model [8], and modified qusicchemical model with quadruplet approximation (MQMQA) [9,10], all of which find applications in CALPHAD modeling of molten salts [11–16]. However, systematically comparing these models and selecting the most appropriate model for molten salts systems remain challenges due to their different physical interpretations and the complexities involved in quantifying model performance.

Several model selection criteria have been employed in computational thermodynamics. For instance, the corrected Akaike information criterion (AICc) [17] has been implemented in open-source software ESPEI [18] facilitate the comparison and selection of Gibbs energy polynomials. Shang et al. [19] utilized AICc to identify optimal models for equations of state fitting. Paulson et al. [20] used Bayes factor [21] to select heat capacity models for the alpha, beta and liquid phases of Hafnium, while Honarmandi et al. [22] used Bayes factor and Bayesian model averaging to

compare models in the Hf-Si system. These studies highlight the utility of statistical comparison methods in guiding model selection within computational thermodynamics.

In the present work, thermodynamic modeling of the LiCl-KCl-LaCl₃ system was performed using experimental data from literature, supplemented with thermochemical data of compounds obtained from density functional theory (DFT) calculations. The open-source software ESPEI [18] and PyCalphad [23] were employed for the modeling process. The recent implementation of MQMQA [24] facilitates Bayesian parameter estimation, uncertainty quantification (UQ) and Bayesian model selection in molten salts modeling [16]. Four candidate models for KCl-LaCl₃ liquid phase were evaluated and compared in the present work. The optimal model for this system is identified using Bayes factor, leading to further optimization of the ternary LiCl-KCl-LaCl₃ system, which demonstrated excellent agreement with experimental data reported in the literature. The present work compares liquid models commonly used in CALPHAD modeling, providing insights into effective model selection strategies.

2 Literature review of the KCl-LaCl₃ and LiCl-KCl-LaCl₃ system

The LiCl-KCl-LaCl₃ system contains the liquid phase, three binary compounds, i.e., LiCl, KCl, and LaCl₃, and two ternary compounds, i.e., K₂LaCl₅ and K₃La₅Cl₁₈ as summarized by Hao et al. [14]. K₂LaCl₅ was reported with a Pnma structure measured by Meyer et al. [25]. Seifert et al. [26] determined the structure of K₃La₅Cl₁₈ with a space group of P6₃/m through X-ray diffraction. The formation enthalpy of K₂LaCl₅ and K₃La₅Cl₁₈ were measured by Seifert et al. [26] using solution calorimetry. Reuter and Seifert reported the heat capacity of K₂LaCl₅ and K₃La₅Cl₁₈ using differential scanning calorimetry (DSC) [27]. Gaune-Escard and Rycerz [28] also measured the heat capacity of K₃La₅Cl₁₈ using DSC. Papatheodorou and Ostvold [29] reported mixing enthalpy in the KCl-LaCl₃ through calorimetric experiments. Qiao et al. [30] utilized DTA techniques to determine melting and phase transition temperatures. In the KCl-LaCl₃, Song and Zheng [31] measured liquidus by DTA. Seifert et al. [26] performed DTA and measured phase boundary data in the LaCl₃ rich composition range.

In the ternary LiCl-KCl-LaCl₃ system, Bagri and Simpson [32] and Samin et al. [33] provided activity coefficient data for LaCl₃ in molten LiCl-KCl eutectic salt using electromotive force measurements and cyclic voltammetry, respectively. Regarding the phase diagram, Song and Zheng [31] reported the liquidus projection and six isopleths. Two research work, by Nakamura et al. [34] and Venkata Krishnan et al. [35], constructed the pseudo-binary phase diagram from LiCl-KCl eutectic to 25 mol% of LaCl₃ in the LiCl-KCl eutectic through DSC. **Mixing enthalpy**.

3 Methodology

3.1 DFT-based first-principles calculations

3.1.1 Helmholtz energy at finite temperatures

The Helmholtz energy $F(V, T)$ as a function of volume (V) and temperature (T) in terms of the DFT-based quasiharmonic approximation (QHA) can be determined by [36],

$$F(V, T) = E(V) + F_{el}(V, T) + F_{vib}(V, T) \quad \text{Eq. 1}$$

where the first term $E(V)$ is static energy at 0 K without the zero-point vibrational energy. In the present work, a four-parameter Birch-Murnaghan (BM4) equation of state (EOS) [36] as shown in **Eq. 2** was used to obtain equilibrium properties at zero external pressure ($P = 0$ GPa), including the static energy E_0 , volume (V_0), bulk modulus (B_0), and its pressure derivate (B').

$$E(V) = a + bV^{-2/3} + cV^{-4/3} + dV^{-2} \quad \text{Eq. 2}$$

where a , b , c , and d are fitting parameters. The second term in **Eq. 1**, $F_{el}(V, T)$, represents the temperature-dependent thermal electronic contribution [37],

$$F_{el}(V, T) = E_{el}(V, T) - T \cdot S_{el}(V, T) \quad \text{Eq. 3}$$

where E_{el} and S_{el} are the internal energy and entropy of thermal electron excitations, respectively, which can be obtained by the electronic density of states (DOS). Note that the thermal electronic contribution to Helmholtz free energy is negligible for non-metal, considering the Fermi level lies in the band gap. The third term in **Eq. 1**, $F_{vib}(V, T)$, represents the vibrational contribution [37,38],

$$F_{vib}(V, T) = k_B T \sum_q \sum_j \ln \left\{ 2 \sinh \left[\frac{\hbar \omega_j(q, V)}{2k_B T} \right] \right\} \quad \text{Eq. 4}$$

where $\omega_j(q, V)$ represents the frequency of the j^{th} phonon mode at wave vector q and volume V , and \hbar the reduced Plank constant.

3.1.2 Details of first-principles calculations

All DFT-based first-principles and phonon calculations in the present work were performed by the Vienna *Ab initio* Simulation Package (VASP) [39]. The projector augmented-wave method (PAW) was used to account for electron-ion interactions in order to increase computational efficiency compared with the full potential methods [40,41]. Electron exchange and correlation effects were described using the generalized gradient approximation (GGA) as implemented by Perdew, Burke, and Ernzerhof (PBE) [42]. The plane-wave basis cutoff energy was 262 eV for relaxations and 520 eV for the final static calculations. The convergence criterion of electronic self-consistency was set as 5×10^{-6} eV/atom for relaxations and static calculations. Seifert et al. [26] reported the structure of $\text{K}_3\text{La}_5\text{Cl}_{18}$ with space group $\text{P}6_3/\text{m}$ with three Wyckoff sites 2b, 2c, and 6h. However, the occupancy of the 2b site is less than 1, while the 2c site is occupied by both K and La atoms. Considering this, ATAT [43] was used to search for all possible configurations under this condition and 9 symmetry inequivalent configurations were found. The configuration with the lowest energy was confirmed using DFT calculations. The phonon calculations were performed using the

supercell method. Table 1 provides detailed parameters for first-principles and phonon calculations, including reciprocal k-points meshes and supercell sizes for phonon calculations.

3.2 CALPHAD modeling

3.2.1 Compounds

In the present work, the ternary compounds in the LiCl-KCl-LaCl₃ system are considered as stoichiometric compounds, including K₂LaCl₅ and K₃La₅Cl₁₈ (as listed in Sec.2). The thermodynamic functions of the binary endmembers KCl and LaCl₃, are sourced from the JANAF tables [44] and SSUB database [45]. The Gibbs energy is expressed as:

$$G_m = \Delta_f H_m^0(298.15) - T S_m^0(298.15) + \int_{298.15}^T C_{P,m} dT - T \int_{298.15}^T \frac{C_{P,m}}{T} dT \quad \text{Eq. 5}$$

where $\Delta_f H_m^0(298.15)$ represents standard formation enthalpy, $S_m^0(298.15)$ denotes the standard entropy at 298.15 K, and $C_{P,m}$ represents the heat capacity. For ternary compounds, their thermodynamic data including enthalpy, entropy, and heat capacity are obtained through DFT-based first-principles and phonon calculations, as detailed in Sec.4.1.

3.2.2 Four models for liquid phase in KCl-LaCl₃

Regarding the liquid phase, we consider four models as candidates to describe complex molten salts: the associate model [7], the two-sublattice ionic model [8], and the MQMQA [9,10] (two sets of coordination numbers).

Species KCl and LaCl₃ are assumed using associate model [7], since lacking observations of other complex associates from literature. The Gibbs energy of the liquid phase can be expressed as:

$$G_m = y_{KCl} {}^oG_{KCl}^{Liquid} + y_{LaCl_3} {}^oG_{LaCl_3}^{Liquid} + RT(y_{KCl} \ln y_{KCl} + y_{LaCl_3} \ln y_{LaCl_3}) \quad \text{Eq. 6}$$

$$+ y_{KCl} y_{LaCl_3} \sum_{v=0} L_{KCl,LaCl_3}^v (y_{KCl} - y_{LaCl_3})^v$$

where y_i is the mole fraction of specie i (=KCl or LaCl₃), ${}^oG_i^{Liquid}$ is the Gibbs energy of species i , R is the gas constant, $L_{KCl,LaCl_3}^v$ is v th the interaction parameter.

Using the two-sublattice ionic model [8], the liquid phase the KCl-LaCl₃ system can be described as:



where cations and anions are separated into two sublattice. The site ratios P and Q are changing in order to maintain charge neutrality:

$$P = y_{Cl^-} = 1 \quad \text{Eq. 8}$$

$$Q = y_{K^+} + y_{La^{3+}} \quad \text{Eq. 9}$$

where y_i represents mole fraction of ion i .

The Gibbs energy function can be expressed as:

$$G_m = y_{K^+} {}^oG_{KCl}^{Liquid} + y_{La^{3+}} {}^oG_{LaCl_3}^{Liquid} + RT(y_{K^+} \ln y_{K^+} + y_{La^{3+}} \ln y_{La^{3+}}) + {}^{xs}G_m \quad \text{Eq. 10}$$

where ${}^{xs}G_m$ represent excess Gibbs energy, which can be expanded based on the Redlich-Kister polynomial [46], similar as in **Eq. 6**:

$${}^{xs}G_m = y_{K^+} y_{La^{3+}} \sum_{v=0} L_{K^+,La^{3+}:Cl^-}^v (y_{K^+} - y_{La^{3+}})^v \quad \text{Eq. 11}$$

where $L_{K^+,La^{3+}:Cl^-}^v$ is v th the interaction parameter.

The MQMQA [9,10] describes the KCl-LaCl₃ liquid phase by assuming interactions between quadruplets, K₂/Cl₂, La₂/Cl₂, and KLa/Cl₂ quadruplets. Coordination numbers Z are defined to describe the second nearest neighbors (SNN) coordination number of the species i ($= K, La, \text{ or } Cl$) in quadruplets. Z of anions can be calculated from **Eq. 12** to maintain charge neutrality as follows:

$$\frac{q_K}{Z_{KLa/ClCl}^{La}} + \frac{q_{La}}{Z_{KLa/ClCl}^{La}} = 2 \times \frac{q_{Cl}}{Z_{AB/ClCl}^{Cl}} \quad \text{Eq. 12}$$

where q_i represents the charges of ion i (= K, La, or Cl). Coordination numbers used in the present work are detailed in

Table 2.

The excess Gibbs energy G^{excess} is related to the formation Gibbs energy of the quadruplet, $\Delta g_{quadruplet}^{ex}$, through the following reaction:



where $\Delta g_{KLa/Cl_2}^{ex}$ represents the Gibbs energy change when forming the quadruplet and can be described by:

$$\Delta g_{KLa/Cl_2}^{ex} = \Delta g_{KLa/Cl_2}^o + \sum_{(i+j) \geq 1} g_{KLa/Cl_2}^{ij} \chi_{KLa/Cl_2}^i \chi_{LaK/Cl_2}^j \quad \text{Eq. 14}$$

where g_{KLa/Cl_2}^{ij} is a function of temperature and is independent of composition. χ_{KLa/Cl_2}^i and χ_{LaK/Cl_2}^j are composition-dependent terms, defined as:

$$\chi_{KLa/Cl_2}^i = \frac{X_{K_2/Cl_2}}{X_{K_2/Cl_2} + X_{KLa/Cl_2} + X_{La_2/Cl_2}} \quad \text{Eq. 15}$$

where X_{KLa/Cl_2} is the fractions of $(KLa/Cl_2)_{quad}$ shown in *Eq. 15*.

All model parameters were simultaneously optimized through the Bayesian approach using the Markov Chain Monte Carlo (MCMC) method [18]. The input data included primarily experimental phase equilibrium data including two or more co-existing phases, mixing enthalpy data, and activity data from literature. For stoichiometric compounds, their thermochemical data from DFT-based calculations were also used as input. In the present work, each model parameter employed two Markov chains with a standard derivation of 0.1 when initializing its Gaussian distribution. During the modeling process, the chain values can be tracked and the MCMC processes were performed until the model parameters converged.

3.3 Bayesian statistics and model selection

ESPEI [18] uses Bayesian parameter estimation to optimize model parameters [47], as shown in:

$$p(\theta|D, M) = \frac{p(D|\theta, M)p(\theta|M)}{p(D|M)} \quad \text{Eq. 16}$$

where θ are the model parameters, M is the model, and D is the input experimental data. In *Eq. 16*, the posterior $p(\theta|D, M)$ is the probability of model parameters conditioned on data, the likelihood $p(D|\theta, M)$ is the probability that the data are described by parameters, the prior $p(\theta|M)$ contains the domain knowledge in the probability distribution of each parameter, and the marginal likelihood (or evidence) $p(D|M)$ is the probability of data being generated by the model.

Bayesian statistics employed in parameter optimization provide a strategy for model selection for CALPHAD modeling [20,22]. Bayes factor usually suggests which model is more favored by the data, which can be evaluated from the ratio of marginal likelihoods for two competing models:

$$K = \frac{p(D|M_1)}{p(D|M_2)} \quad \text{Eq. 17}$$

The marginal likelihood has the desirable qualities of rewarding models that match the data well and penalizing models that are overly complex (i.e., have too many degrees of freedom or parameters). The marginal likelihood is given by:

$$p(D|M) = \int_{\Omega_\theta} p(D|\theta, M)p(\theta|M)d\theta \quad \text{Eq. 18}$$

where Ω_θ represents the complete parameter space. The evaluation of marginal likelihood requires computation of an integral with dimension given by the number of parameters, which is typically high-dimensional. The evaluation of the marginal likelihood $p(D|M)$ is often usually difficult and computationally expensive. The harmonic mean estimator was proposed by Newton and Raftery [48] to estimate the marginal likelihood:

$$p(D|M) \approx \left[\frac{1}{N} \sum_{i=1}^N p(D|\theta_i, M)^{-1} \right]^{-1} \quad \text{Eq. 19}$$

where θ_i are samples from the parameters' prior $p(\theta|M)$. Likelihood values can be obtained from ESPEI MCMC output, which provides opportunities to provide statistical comparison of liquid models through Bayes factor.

4 Results and discussion

4.1 Thermodynamic properties in LiCl-KCl-LaCl₃ by first-principles calculations

Thermodynamic properties of compounds in the KCl-LaCl₃ system were investigated using first-principles calculations. Table 4 summarizes the equilibrium properties of V_0 , B_0 , and B' at 0 K obtained from DFT calculations in comparison with experiments. The present work predicts the B_0 value of KCl to be 16.23 GPa, which is slightly lower than the experimental measurement of 19.7 GPa reported by Norwood et al. [49]. The equilibrium volume of LaCl₃ is predicted to be 27.37 Å³/atom in the present work, which is in good agreement with the value of 26.38 Å³/atom reported by Zachariasen [50]. It indicates that the present DFT calculations provide reliable predictions regarding the equilibrium properties of compounds in the KCl-LaCl₃ system.

Thermodynamic properties at finite temperatures are obtained through phonon calculations. Figure 1 compares the predicted heat capacity (C_p), entropy (S), and enthalpy ($H-H_{300}$) of KCl and LaCl₃ from the phonon-based QHA to the data from the SGTE database [45]. The C_p and $H-H_{300}$ results of KCl show good agreements with SGTE [45], while the difference in S is around 6%. The results

of LaCl_3 show the difference of C_p less than 3.2 J/mol-atom-K at high temperatures, while S and H-H₃₀₀ closely match the results from SGTE [45]. Figure 2 shows the predicted heat capacities C_p of compounds K_2LaCl_5 and $\text{K}_3\text{La}_5\text{Cl}_{18}$ in comparison to experiments [27,28], demonstrating excellent agreement. These results of K_2LaCl_5 and $\text{K}_3\text{La}_5\text{Cl}_{18}$ obtained from the present DFT calculations are then used in subsequent thermodynamic modeling.

4.2 Model selection for the liquid phase in the KCl-LaCl₃ system

The KCl-LaCl₃ system is modeled using four models: the associate model (Associate-M1), the ionic model (Ionic-M2), MQMQA (MQMQA-M3), and MQMQA with different coordination numbers (MQMQA-M4). Table 3 presents details of these models. Each model has four adjustable parameters and has been optimized over at least 1000 MCMC iterations until the model parameters converged. Figure 3 compares the phase diagrams calculated from these four models with experimental data. It shows that in the KCl rich region liquidus, MQMQA-M3 and MQMQA-M4 provide better agreements with experimental data than Associate-M1 and Ionic-M2.

Table 5 lists the detailed invariant reactions predicted by the models in comparison with experimental data [26,31]. In general, all four models show excellent agreements with the experimental data. Ionic-M2 and MQMQA-M4 slightly overpredict invariant temperatures compared to Associate-M1 and MQMQA-M3. Specifically, Ionic-M2 and MQMQA-M4 predict a eutectic temperature of 854 K for the reaction $\text{Liquid} \leftrightarrow \text{KCl} + \text{K}_2\text{LaCl}_5$, which is 9 K higher than

845 K reported by Song et al. [31] and 1 K above 853 K by Seifert et al.[26]. For the melting temperature of K_2LaCl_5 , Ionic-M2 predicts 917 K, while MQMQA-M4 predicts 926 K, both higher than experimental measurements of 913 K by Seifert et al.[26] and 916 K by Song et al. [31]. Associate-M1 slightly underpredicts the peritectic temperature of the reaction $Liquid+LaCl_3 \leftrightarrow K_3La_5Cl_{18}$ at 882 K, which is 3 K lower than 885 K by Seifert et al.[26] and other models. The mean absolute error (MAE) for predicting invariant temperatures using Associate-M1 is 2.5 K. MQMQA-M3 provides good agreements with experimental data, with a slightly lower prediction of the eutectic temperature for the reaction $Liquid \leftrightarrow K_2LaCl_5+K_3La_5Cl_{18}$ at 845 K, which is 6 K lower than 851 K reported by Seifert et al.[26]. Regarding the invariant compositions $x(LaCl_3)$, MQMQA-M3 and MQMQA-M4 offer better predictions with an MAE of 0.017 for both, compared to 0.025 for Associate-M1 and 0.022 for Ionic-M2.

Figure 4 shows the mixing enthalpy of the liquid phase at 1173 K calculated using four models. These results are compared with the experimental data provided by Papatheodorou and Ostvold [29]. The comparison indicates that Associate-M1 and Ionic-M2 predict lower mixing enthalpy values than MQMQA-M3 and MQMQA-M4. Notably, Associate-M1 and Ionic-M2 align more closely with experimental data [29], particularly in the composition region where $x(LaCl_3) > 0.4$.

Each model demonstrates particular strengths in predicting thermodynamic properties of the KCl- $LaCl_3$. Associate-M1 and Ionic-M2 perform well in predicting mixing enthalpy, showing a better

match with experimental data. However, these models are less accurate in predicting phase boundaries compared to MQMQA-M3 and MQMQA-M4. The choice of an appropriate model remains a challenge, as it requires balancing agreement with all available experimental data. A quantitative method is needed to determine the overall favorability of a model based on the data.

Bayesian parameter estimation through MCMC offers a powerful tool to statistically compare models, as demonstrated in Sec.3.3. In the present work, the last 600 iterations from MCMC were used to compute the marginal likelihood $p(D|M)$ for each model. Table 6 lists the estimated marginal likelihood value for each model, indicating that MQMQA-M3 has the highest marginal likelihood value of $\ln(p(D|M_3)) = -370.628$. Consequently, the Bayes factors for the other models were calculated relative to MQMQA-M3, using marginal likelihood value of MQMQA-M3 as the numerator in *Eq. 17*. The interpretation of the Bayes factor is also included in Table 6 according to the guidelines of Kass and Raftery [21]. The results indicate that the marginal likelihoods of Ionic-M2 $\ln(p(D|M_2)) = -373.410$ and MQMQA-M4 $\ln(p(D|M_4)) = -371.420$ are close to that of MQMQA-M3. In contrast, the marginal likelihood of Associate-M1 $\ln(p(D|M_1)) = -439.135$ is significantly lower than that of MQMQA-M3, indicating that the Associate-M1 model is considerably less favorable compared to the other three models. The Bayes factor $\log_{10}K_{M3/M1}$ is 29.752, suggesting decisive evidence of favoring MQMQA-M3 over Associate-M1. This is due to the larger discrepancy in phase boundary predictions from Associate-M1 compared to the experimental phase diagram data shown in Figure 3(a). Regarding the Ionic-M2, the Bayes factor $\log_{10}K_{M3/M2} = 1.208$ indicates strong evidence of favoring MQMQA-M3 over Ionic-M2.

Additionally, the Bayes factor comparing two MQMQA models, $\log_{10}K_{M3/M4}$, is 0.344, suggesting that MQMQA-M3 is slightly favored over MQMQA-M4, but not worth a bare mention when comparing these two models. It implies that the choice of these two sets of coordination numbers did not significantly affect the performance of MQMQA models in predicting thermodynamic properties in KCl-LaCl₃ systems.

In summary, Bayesian parameter estimation through MCMC indicates that MQMQA-M3 is more favored by the input thermodynamic data, including phase boundary and mixing enthalpy data, over the other three models. This approach provides robust techniques for estimating the marginal likelihood values to assess the probability of data being generated by the model, as well as calculating Bayes factors to statistically compare different models.

4.3 Thermodynamic modeling of the LiCl-KCl-LaCl₃ system

The MQMQA-M3 is selected for the KCl-LaCl₃ system according to the Bayes factor. The ternary LiCl-KCl-LaCl₃ system is further improved. The other two binary systems LiCl-KCl and LiCl-LaCl₃ are taken from MSTDB-TC [15]. The available experimental data used for the optimization includes phase boundary data measured by Nakamura et al. [34] and Venkata Krishnan et al. [35], activity data measured by Bagri and Simpson [32] and Samin et al. [33], and mixing enthalpy of LaCl₃ in LiCl-KCl eutectic. **Error! Reference source not found.** lists the ternary interaction parameters after MCMC optimization.

Thermodynamic properties predicted from the present modeling are compared with available experimental data. In addition, uncertainty quantification is performed to propagate parameter uncertainties into property predictions. Figure 5(a) presents the activity of LaCl_3 in eutectic LiCl-KCl at 773 K, compared with measurements by Bagri et al. [32] and Samin et al. [33]. The present modeling aligns more closely with results by Bagri et al. [32], due to they provided a larger data set over a broader composition range than Samin et al. [33]. The model shows good agreement in the low $x(\text{LaCl}_3)$ region ($x(\text{LaCl}_3) < 0.015$) but slightly overestimates the activity when $x(\text{LaCl}_3)$ increases to 0.02. Compared to previous modeling work, the current model represents a significant improvement over Hao et al. [14] in predicting the activity. MSTDB-TC [15] shows good agreement in the composition range of $x(\text{LaCl}_3)$ from 0.022 to 0.027. Uncertainty quantification was performed using the last 10 MCMC iterations with 60 MCMC samples. Figure 5(b) illustrates the uncertainty in predicting activity, with a 95% credible interval. It shows that the uncertainty range is below the final prediction and is larger when increasing $x(\text{LaCl}_3)$. This indicates that the current model has an uncertainty to predict lower activity values, particularly at higher $x(\text{LaCl}_3)$ values.

Figure 6 shows the mixing enthalpy calculations at 873 K and 1133 K from the present modeling, in comparison with experimental data and modeling by Hao et al. [14] and MSTDB-TC [15]. In Figure 6(a), at 873 K, all three modeling work closely match experimental measurements for $x(\text{LaCl}_3) < 0.2$, while showing different curve shapes in LaCl_3 rich regions. The present modeling

predicts a minimum energy similar to that of MSTDB-TC [15], whereas Hao et al. [14] predicts an around 600 J/mol lower mixing enthalpy. Experiments investigations at 1133 K primarily focus on LaCl_3 rich regions. Figure 6(b) indicates that both Hao et al. [14] and MSTDB-TC [15] predict lower mixing enthalpy compared to the present modeling and experiments. The present work improves the accuracy of mixing enthalpy predictions, reducing the MAE to 45.84 J/mol, compared to 159.75 J/mol by Hao et al. [14] and 183.30 J/mol by MSTDB-TC [15]. Figure 6(c) presents the uncertainty quantification of the present modeling in predicting mixing enthalpy, represented by the 95% credible interval. At 1133 K, all existing experimental data fall within the lower boundary of the uncertainty region. This implies that our current modeling might underestimate the mixing enthalpy, particularly around $x(\text{LaCl}_3) = 0.4$. Further experimental or simulation studies in this composition range are recommended to enhance the accuracy of our modeling.

Figure 7 presents the partial isopleth between the eutectic KCl-LiCl and LaCl_3 calculated from the present modeling compared with experimental measurements [34,35], demonstrating a close match of liquidus and solidus lines. For the eutectic reaction $\text{Liquid} \leftrightarrow \text{KCl} + \text{LiCl} + \text{K}_2\text{LaCl}_5$, the present modeling predicts a eutectic temperature of 630 K, which is 5 K higher than the values of 625 K reported by Nakamura et al. [34] and Venkata Krishnan et al. [35]. Similarly, for the reaction $\text{Liquid} \leftrightarrow \text{LiCl} + \text{K}_2\text{LaCl}_5 + \text{K}_3\text{La}_5\text{Cl}_{18}$, the present modeling predicts the eutectic temperature at 705 K, 3 K higher than the reported values of 702 K by Nakamura et al. [34] and Venkata Krishnan et

al. [35]. Overall, the present modeling of LiCl-KCl-LaCl₃ systems demonstrates good agreement with experimental data [32–35] regarding thermodynamic properties.

5 Conclusions

The present work demonstrates an application of Bayesian model selection strategies to select optimal model for molten salts, focusing on the KCl-LaCl₃ system. Four candidate models are considered: the associate model, two-sublattice ionic model, and MQMQA with two sets of coordination numbers. By estimating marginal likelihoods of each model from MCMC optimization and calculating Bayes factor to compare models, one of the MQMQA models is suggested as the most favorable for describing the KCl-LaCl₃ system based on available input data. Additionally, DFT calculations provide important thermodynamic properties for compounds in the KCl-LaCl₃, including equilibrium volumes, bulk moduli, enthalpies, entropies, and heat capacities. Furthermore, the ternary LiCl-KCl-LaCl₃ system is optimized, demonstrating better agreements with experimental data compared to previous modeling in the literature. The uncertainty quantification and propagation show that the present modeling provides reliable prediction of activity and mixing enthalpy when compared with experimental data. This Bayesian model selection approach facilitates a more rational comparison between liquid models and advances the optimization process, enhancing the accuracy of thermodynamic predictions in molten salts.

Acknowledgments

The authors acknowledge financial supports by the U.S. Department of Energy, Office of Nuclear Energy's Nuclear Energy University Programs via Award No. DE-NE0009288. First-principles calculations were performed partially on the Roar supercomputer at the Pennsylvania State University's Institute for Computational and Data Sciences (ICDS), partially on the resources of the National Energy Research Scientific Computing Center (NERSC) supported by the U.S. Department of Energy, Office of Science User Facility operated under Contract No. DE-AC02-05CH11231, and partially on the resources of ACCESS (previously the Extreme Science and Engineering Discovery Environment, XSEDE) supported by National Science Foundation (NSF) with Grant No. ACI-1548562.

6 Figures and Figure Captions

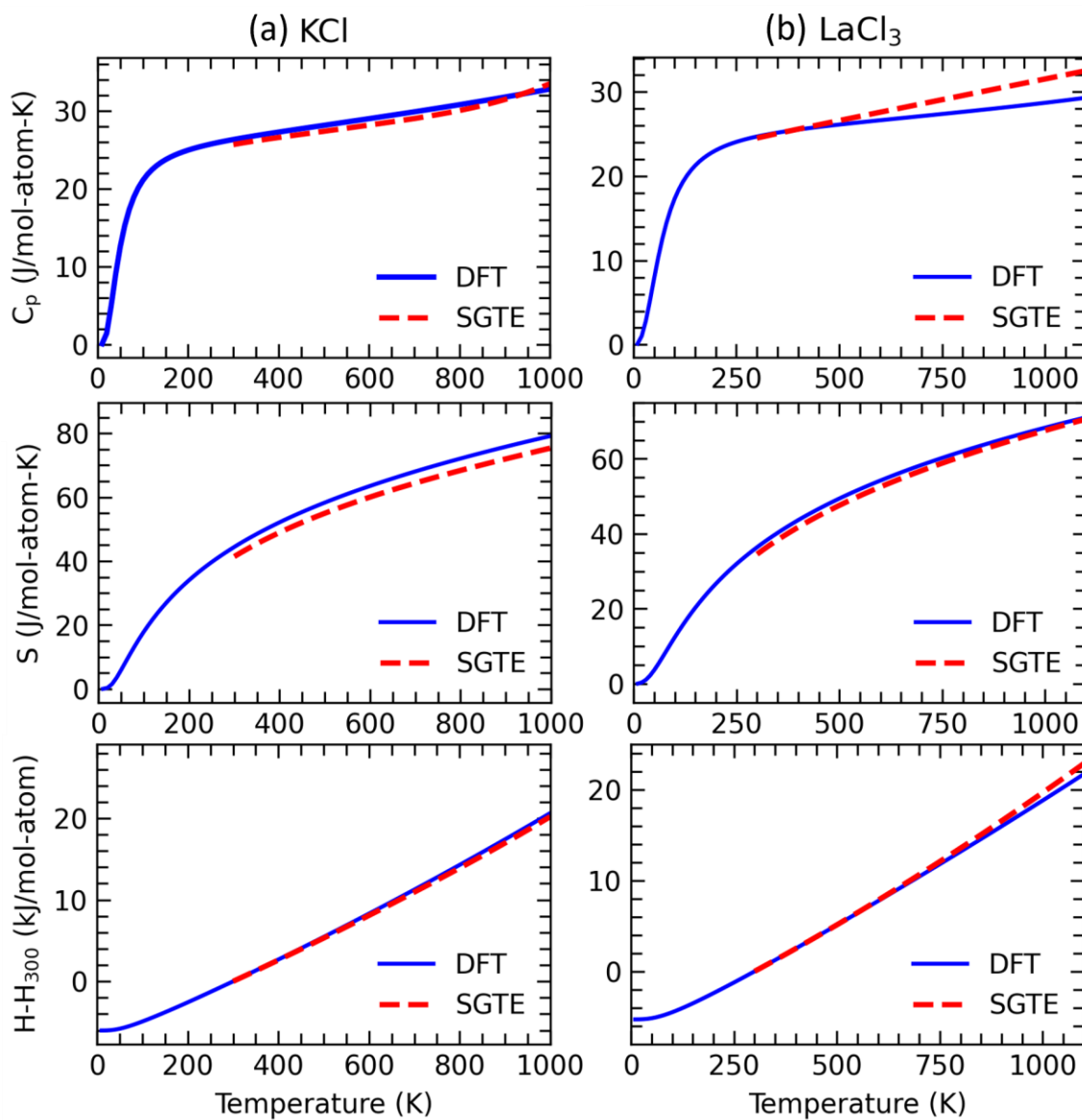


Figure 1. Comparison of heat capacity C_p , entropy S and enthalpy with reference at 300 K ($H-H_{300}$) of (a) KCl and (b) LaCl₃ from the DFT-based phonon calculations (blue lines) with the SGTE data [45] (red dash lines).

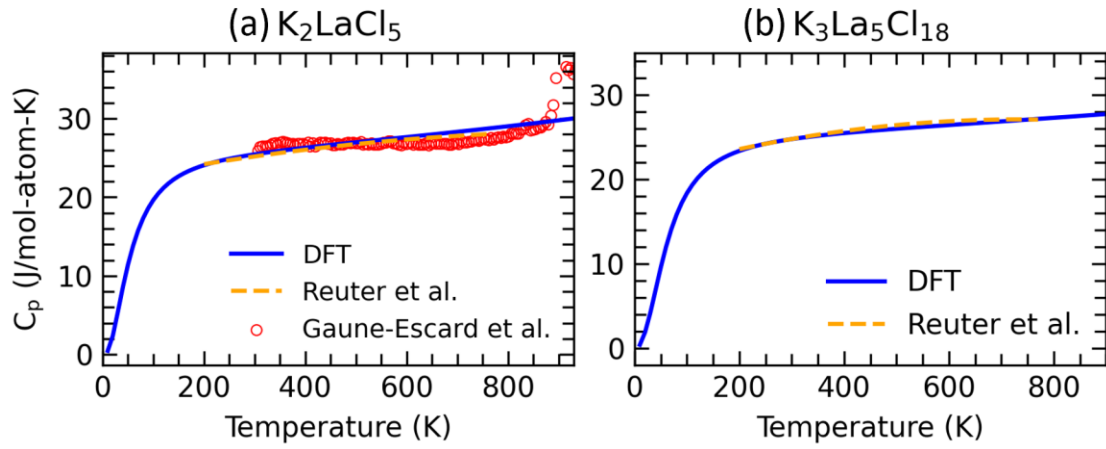


Figure 2. Comparison of heat capacity C_p (a) K_2LaCl_5 and (b) $K_3La_5Cl_{18}$ from the DFT-based phonon calculations (blue lines) with experiments by Reuter et al. [27] (yellow dash lines) and Gaune-Escard et al. [28] (red circles).

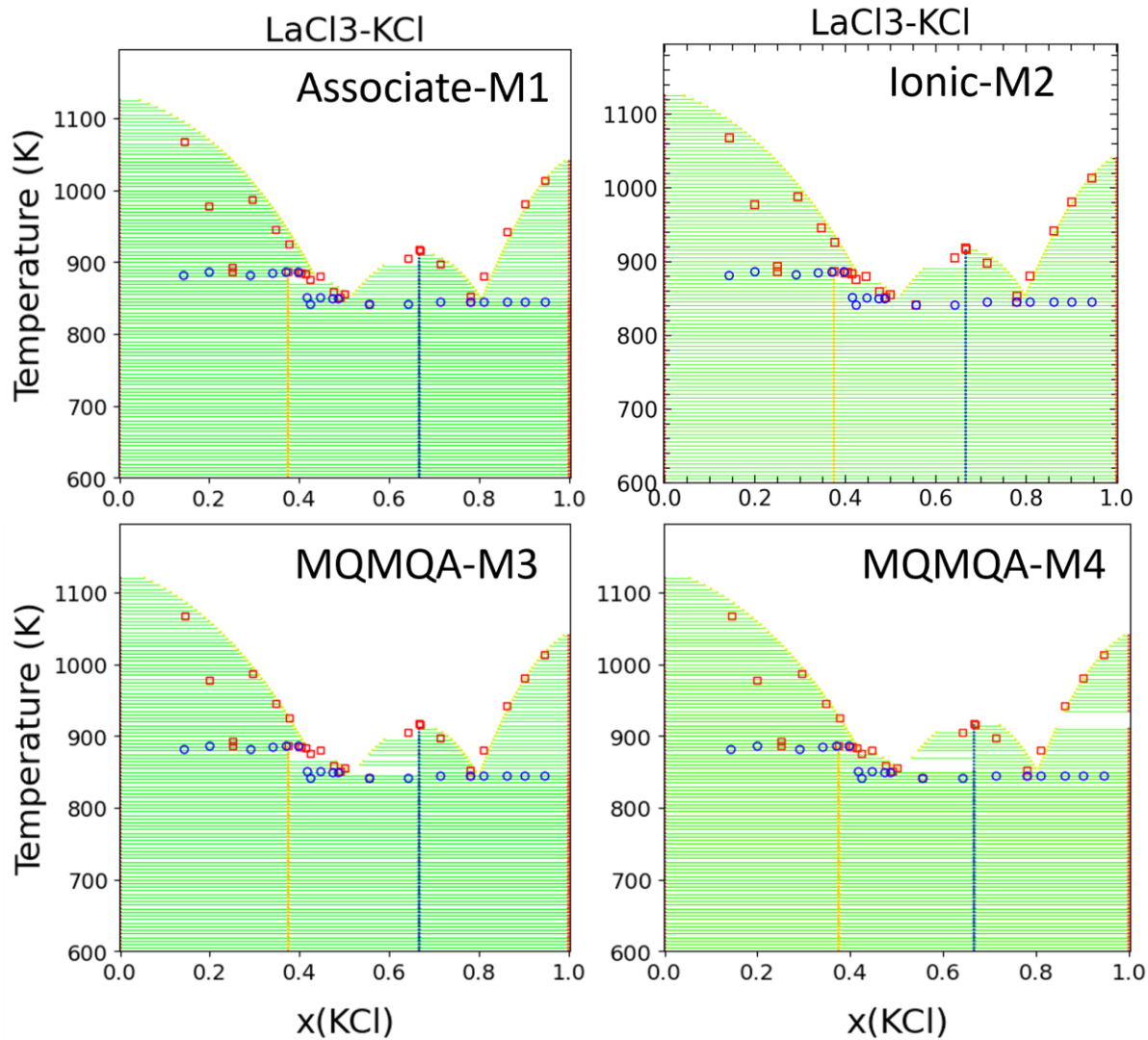


Figure 3. Phase diagrams of LaCl₃-KCl system with the liquid phase modeled using (a) associate model (Associate-M1), (b) ionic model (Ionic-M2), (c) MQMQA (MQMQA-M3), and (d) MQMQA (MQMQA-M4) in comparison to experimental data.

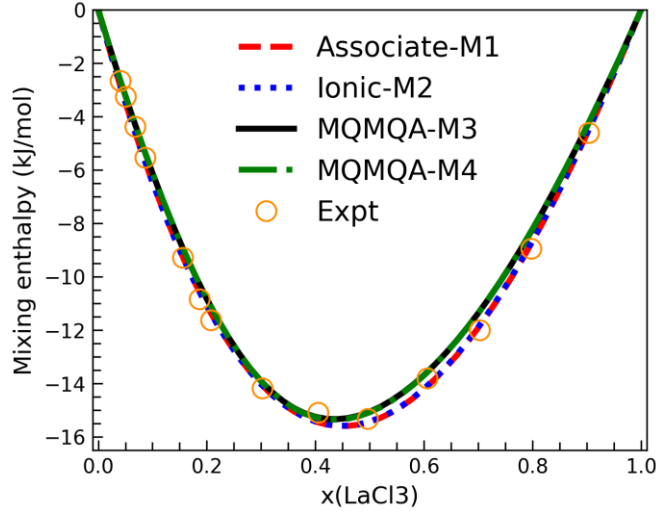


Figure 4. Mixing enthalpy of $\text{LaCl}_3\text{-KCl}$ liquid phase at 1173K calculated from four models in comparison to experimental data by Papatheodorou and Ostvold [29], red dash line represents Associate-M1, blue dotted line represents Ionic-M2, black solid line represents MQMQA-M3, and green dash dotted line represents MQMQA-M4.

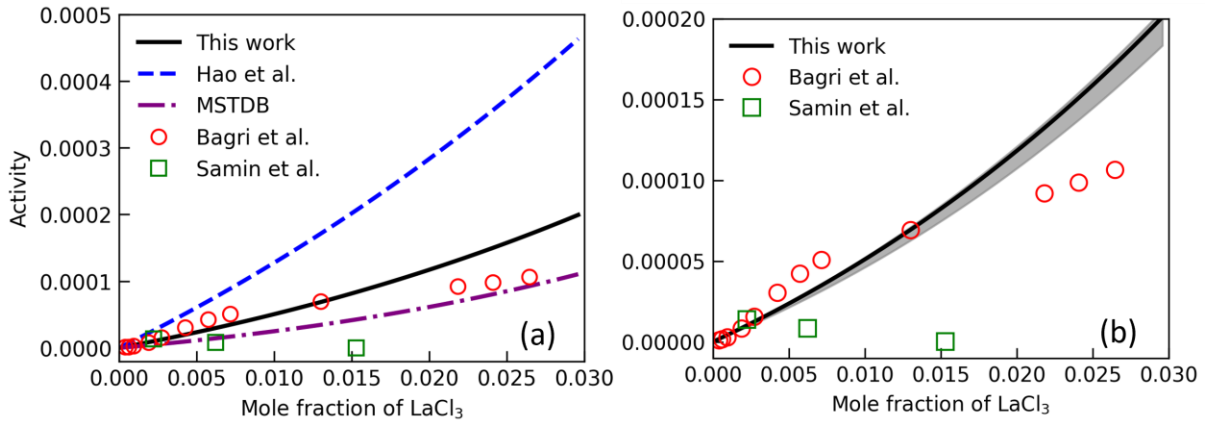


Figure 5. (a) Activity of LaCl_3 in KCl-LiCl eutectic at 773 K calculated from the present modeling in comparison to modeling work from Hao et al. [14] (blue dash line) and MSTDB-TC [15] (purple dash dotted line), experimental measurements by Bagri et al. (red circles) and Samin et al. (green squares). (b) The uncertainty of the present modeling in predicting activity shown in grey region using 95% credible interval. in predicting the activity.

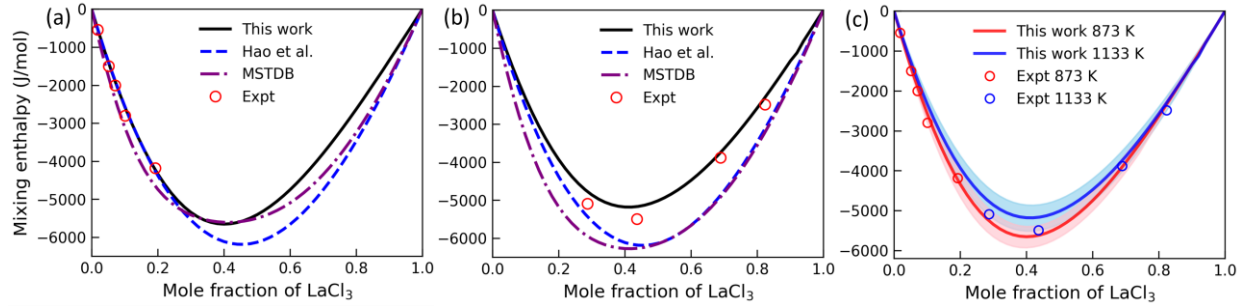


Figure 6. Mixing enthalpy in LiCl-KCl-LaCl₃ at (a) 873 K and (b) 1133 K calculated from the present modeling compared with experimental measurements and previous modeling work by Hao et al. [14] and MSTDB-TC [15]. (c) The uncertainty of the present modeling in predicting mixing enthalpy shown in light red region (for 873 K) and light blue region (for 1133 K) using 95% credible interval.

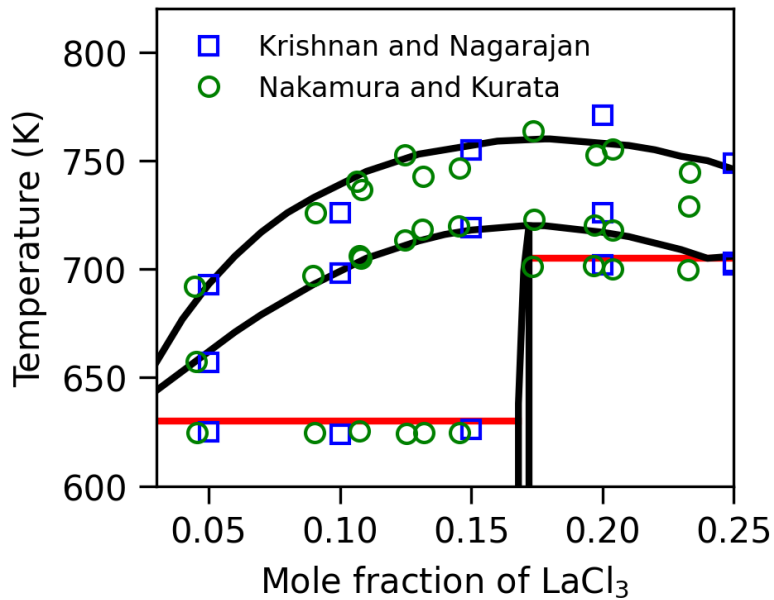


Figure 7. Partial isopleth between eutectic KCl-LiCl and LaCl₃ calculated from this work in comparison to experimental measurements by Krishnan and Nagarajan (blue squares) and Nakamura and Kurata (green circles).

7 Tables and Table Captions

Table 1. Details of DFT-based first-principles and phonon calculations for each compound, including space group, total atoms in the supercells, k-point meshes for structure relaxations and the final static calculations (indicated by DFT), supercell sizes for phonon calculations, k-point meshes for phonon calculations.

Phase	Space Group	Atoms in crystallographic cell	k-points for DFT	Atoms in supercell for phonon	k-points for phonon
KCl	Fm $\bar{3}$ m	8	8×8×8	64	3×3×3
LaCl ₃	P6 ₃ /m	8	8×8×12	64	2×2×2
K ₂ LaCl ₅	Pnma	32	7×7×4	32	4×4×2
K ₃ La ₅ Cl ₁₈	P3	26	8×8×5	26	5×5×3

Table 2. Coordination number used in the present CALPHAD modeling work with MQMQA for the liquid phase.

A	B		$Z_{AB/ClCl}^A$	$Z_{AB/ClCl}^B$	$Z_{AB/ClCl}^F$
K ⁺	K ⁺		6.0	6.0	6.0
La ³⁺	La ³⁺		6.0	6.0	2.0
K ⁺	La ³⁺	MQMQA-M3	2.0	6.0	2.0
		MQMQA-M4	3.5	6.0	2.55

Table 3. Details of four models for KCl-LaCl₃ and model parameters.

Model name	Model details	Model interaction parameters
Associate-M1	(KCl, LaCl ₃)	$L_{KCl,LaCl_3}^0 = -61777.370 + 1.218 * T$ $L_{KCl,LaCl_3}^1 = -12634.241 - 1.383 * T$
Ionic-M2	(K ⁺ , La ³⁺) _P (Cl ⁻) _Q	$L_{K^+,La^{3+}:Cl^-}^0 = -61720.724 + 5.247 * T$ $L_{K^+,La^{3+}:Cl^-}^1 = -12786.004 + 3.360 * T$
MQMQA-M3	See Table 2	$\Delta g_{KLa/Cl_2}^{ex} = -13295.794 - 1.236 * T$ $+ (-9228.101)\chi_{KLa/Cl_2}$ $+ (-2071.866)\chi_{LaK/Cl_2}$
MQMQA-M4	See Table 2	$\Delta g_{KLa/Cl_2}^{ex} = -13313.121 - 1.333 * T$ $+ (-9173.701)\chi_{KLa/Cl_2}$ $+ (-1989.647)\chi_{LaK/Cl_2}$

Table 4. Predicted equilibrium properties of volume V₀, bulk modulus B₀, and first derivative of bulk modulus with respect to pressure B' for compounds in the KCl-LaCl₃ system based on the present EOS fitting at 0 K (*Eq. 2*). Experimental data are also listed for comparison.

Compounds	V ₀ (Å ³ /atom)	B ₀ (GPa)	B'	References
KCl	32.62	16.23	4.67	This work
		19.7		Norwood et al. [49]
LaCl ₃	27.37	29.02	6.40	This work
	26.38			Zachariasen [50]
K ₂ LaCl ₅	29.96	15.89	5.38	This work
K ₃ La ₅ Cl ₁₈	27.49	26.46	6.35	This work

Table 5. Predicted invariant equilibria in the KCl-LaCl₃ system by the four models, compared with experimental data.

Reaction		x(LaCl ₃)	Temperature (K)	Source
Eutectic	Liquid \leftrightarrow KCl+K ₂ LaCl ₅	0.22	853	Seifert et al.[26]
		0.22	845	Song et al. [31]
		0.197	848	Associate-M1
		0.202	854	Ionic-M2
		0.204	847	MQMQA-M3
		0.200	854	MQMQA-M4
		Melting	Liquid \leftrightarrow K ₂ LaCl ₅	0.333
0.333	916			Song et al. [31]
0.333	913			Associate-M1
0.333	917			Ionic-M2
0.333	915			MQMQA-M3
0.333	926			MQMQA-M4
Eutectic	Liquid \leftrightarrow K ₂ LaCl ₅ +K ₃ La ₅ Cl ₁₈			0.51
		0.485	852	Associate-M1
		0.481	851	Ionic-M2
		0.482	845	MQMQA-M3
		0.49	851	MQMQA-M4
Peritectic	Liquid+LaCl ₃ \leftrightarrow K ₃ La ₅ Cl ₁₈	0.595	885	Seifert et al.[26]
		0.565	882	Associate-M1
		0.573	885	Ionic-M2
		0.586	885	MQMQA-M3
		0.586	885	MQMQA-M4

Table 6. The marginal likelihood of each model, Bayes factor calculated comparing MQMQA-M3 with each model, and strength of evidence according to Kass and Raftery [21].

Model name	Marginal likelihood (ln value)	Bayes factor $\log_{10}K$	Strength of evidence
Associate-M1	-439.135	29.752	Decisive
Ionic-M2	-373.410	1.208	Strong
MQMQA-M3	-370.628	-	-
MQMQA-M4	-371.420	0.344	Not worth more than a bare mention

Table 7. Ternary interaction parameters in the LiCl-KCl-LaCl₃ liquid phase using MQMQA after MCMC optimization.

System	Ternary interaction parameters
LiCl-KCl-LaCl ₃	$\Delta g_{\text{LaLi(K)/Cl}_2}^{101} = 10153.591$ $\Delta g_{\text{KLi(La)/Cl}_2}^{001} = 18921.383 - 12.806 * T$

8 References

- [1] K. Sridharan, T. Allen, M. Anderson, M. Simpson, Thermal Properties of LiCl-KCl Molten Salt for Nuclear Waste Separation, (2012). <https://doi.org/10.2172/1058922>.
- [2] A. Mourogov, P.M. Bokov, Potentialities of the fast spectrum molten salt reactor concept: REBUS-3700, *Energy Convers. Manag.* 47 (2006) 2761–2771. <https://doi.org/10.1016/J.ENCONMAN.2006.02.013>.
- [3] M. Iizuka, T. Koyama, N. Kondo, R. Fujita, H. Tanaka, Actinides recovery from molten salt/liquid metal system by electrochemical methods, *J. Nucl. Mater.* 247 (1997) 183–190. [https://doi.org/10.1016/S0022-3115\(97\)00096-2](https://doi.org/10.1016/S0022-3115(97)00096-2).
- [4] Z.K. Liu, Computational thermodynamics and its applications, *Acta Mater.* 200 (2020) 745–792. <https://doi.org/10.1016/J.ACTAMAT.2020.08.008>.
- [5] H.L. Lukas, S.G. Fries, B. Sundman, *Computational Thermodynamics: the Calphad Method*, Cambridge University Press, Cambridge UK, 2007. <https://iopscience.iop.org/article/10.1088/0305-4470/27/7/011>.
- [6] Z.-K. Liu, Y. Wang, *Computational thermodynamics of materials*, Cambridge University Press, 2016.
- [7] F. Sommer, Association Model for the Description of the Thermodynamic Functions of Liquid Alloys: I. Basic Concepts, *Int. J. Mater. Res.* 73 (1982) 72–76. <https://doi.org/10.1515/IJMR-1982-730202>.
- [8] M. Hillert, B. Jansson, B. Sundman, J. ågren, A two-sublattice model for molten solutions with different tendency for ionization, *Metall. Trans. A.* 16 (1985) 261–266. <https://doi.org/10.1007/BF02815307>.
- [9] A.D. Pelton, P. Chartrand, G. Eriksson, The modified quasi-chemical model: Part IV. Two-sublattice quadruplet approximation, *Metall. Mater. Trans. A* 2001 326. 32 (2001) 1409–1416. <https://doi.org/10.1007/S11661-001-0230-7>.
- [10] A.D. Pelton, *Phase diagrams and thermodynamic modeling of solutions*, Elsevier, 2014.
- [11] L. Rycerz, J. Kapala, B. Salamon, I. Szczygieł, M. Gaune-Escard, Phase diagram and thermodynamic properties of the LaI₃-RbI binary system, *Calphad.* 70 (2020) 101809. <https://doi.org/10.1016/J.CALPHAD.2020.101809>.
- [12] L. Rycerz, J. Kapala, M. Gaune-Escard, Experimental mixing enthalpy and thermodynamic modelling of UCl₃-KCl system, *J. Mol. Liq.* 342 (2021) 116963. <https://doi.org/10.1016/J.MOLLIQ.2021.116963>.
- [13] W. Zhou, Y. Wang, J. Zhang, M. Khafizov, Calculated thermodynamic properties of GdCl₃ in LiCl-KCl eutectic molten salt, *J. Nucl. Mater.* 508 (2018) 40–50. <https://doi.org/10.1016/J.JNUCMAT.2018.05.030>.

- [14] L. Hao, S. Sridar, W. Xiong, Thermodynamic optimization of KCl-LiCl-LaCl₃ with ionic two-sublattice model for liquid, *J. Mol. Liq.* 400 (2024) 124516. <https://doi.org/10.1016/J.MOLLIQ.2024.124516>.
- [15] J.C. Ard, J.A. Yingling, K.E. Johnson, J. Schorne-Pinto, M. Aziziha, C.M. Dixon, M.S. Christian, J.W. McMurray, T.M. Besmann, Development of the Molten Salt Thermal Properties Database – Thermochemical (MSTDB-TC), example applications, and LiCl-RbCl and UF₃-UF₄ system assessments, *J. Nucl. Mater.* 563 (2022) 153631. <https://doi.org/10.1016/j.jnucmat.2022.153631>.
- [16] R. Gong, S.L. Shang, Y. Wang, J. Paz Soldan Palma, H. Kim, Z.K. Liu, Revisiting thermodynamics in (LiF, NaF, KF, CrF₂)-CrF₃ by first-principles calculations and CALPHAD modeling, *Calphad.* 85 (2024) 102703. <https://doi.org/10.1016/J.CALPHAD.2024.102703>.
- [17] J.E. Cavanaugh, Unifying the derivations for the Akaike and corrected Akaike information criteria, *Stat. Probab. Lett.* 33 (1997) 201–208. [https://doi.org/10.1016/S0167-7152\(96\)00128-9](https://doi.org/10.1016/S0167-7152(96)00128-9).
- [18] B. Bocklund, R. Otis, A. Egorov, A. Obaied, I. Roslyakova, Z.K. Liu, ESPEI for efficient thermodynamic database development, modification, and uncertainty quantification: Application to Cu-Mg, *MRS Commun.* 9 (2019) 618–627. <https://doi.org/10.1557/mrc.2019.59>.
- [19] S.-L. Shang, R. Gong, M.C. Gao, D.C. Pagan, Z.-K. Liu, Revisiting first-principles thermodynamics by quasiharmonic approach: Application to study thermal expansion of additively-manufactured Inconel 625, *Scr. Mater.* 250 (2024) 116200. <https://doi.org/10.1016/J.SCRIPTAMAT.2024.116200>.
- [20] N.H. Paulson, E. Jennings, M. Stan, Bayesian strategies for uncertainty quantification of the thermodynamic properties of materials, *Int. J. Eng. Sci.* 142 (2019) 74–93. <https://doi.org/10.1016/j.ijengsci.2019.05.011>.
- [21] R.E. Kass, A.E. Raftery, Bayes Factors, *J. Am. Stat. Assoc.* 90 (1995) 773–795. <https://doi.org/10.1080/01621459.1995.10476572>.
- [22] P. Honarmandi, T.C. Duong, S.F. Ghoreishi, D. Allaire, R. Arroyave, Bayesian uncertainty quantification and information fusion in CALPHAD-based thermodynamic modeling, *Acta Mater.* 164 (2019) 636–647. <https://doi.org/10.1016/j.actamat.2018.11.007>.
- [23] R. Otis, Z.-K. Liu, pycalphad: CALPHAD-based Computational Thermodynamics in Python, *J. Open Res. Softw.* 5 (2017) 1–11. <https://doi.org/10.5334/jors.140>.
- [24] J. Paz Soldan Palma, R. Gong, B.J. Bocklund, R. Otis, M. Poschmann, M. Piro, S. Shahbazi, T.G. Levitskaia, S. Hu, N.D. Smith, Y. Wang, H. Kim, Z.-K. Liu, S.-L. Shang, Thermodynamic modeling with uncertainty quantification using the modified quasichemical model in quadruplet approximation: Implementation into PyCalphad and ESPEI, *Calphad.* 83 (2023) 102618. <https://doi.org/10.1016/j.calphad.2023.102618>.
- [25] G. Meyer, E. Hüttel, K₂MCl₅ (M = La—Dy) und Rb₂MCl₅ (M = La—Eu): Ino-Chloride mit siebenfach koordinierten Seltenen Erden, *ZAAC - J. Inorg. Gen. Chem.* 497 (1983) 191–198. <https://doi.org/10.1002/ZAAC.19834970218>.

- [26] H.J. Seifert, H. Fink, G. Thiel, Thermodynamic properties of double chlorides in the systems ACl/LaCl_3 ($A \equiv \text{Na, K, Rb, Cs}$), *J. Less-Common Met.* 110 (1985) 139–147. [https://doi.org/10.1016/0022-5088\(85\)90315-7](https://doi.org/10.1016/0022-5088(85)90315-7).
- [27] G. Reuter, H.J. Seifert, The heat capacities of ternary lanthanum chlorides An LaCl_{3+n} from 200 to 770 K and the ΔC_p values for their formation from $n\text{ACl} + \text{LaCl}_3$, *Thermochim. Acta.* 237 (1994) 219–228. [https://doi.org/10.1016/0040-6031\(94\)80178-9](https://doi.org/10.1016/0040-6031(94)80178-9).
- [28] M. Gaune-Escard, L. Rycerz, Heat Capacity of K_3LnCl_6 Compounds with $\text{Ln} = \text{La, Ce, Pr, Nd}$, *Zeitschrift Fur Naturforsch. - Sect. A J. Phys. Sci.* 54 (1999) 229–235. <https://doi.org/10.1515/ZNA-1999-3-412/MACHINEREADABLECITATION/RIS>.
- [29] G.N. Papatheodorou, T. Ostvold, Thermodynamic studies of binary charge unsymmetrical fused salt systems. Calorimetric and electromotive force measurements of liquid lanthanum(III) chloride-alkali chloride mixtures, *J. Phys. Chem.* 78 (1974) 181–185. <https://doi.org/10.1021/j100595a019>.
- [30] Z. Qiao, M. Wang, C. Zheng, S. Duan, Measurement and Calculation of $\text{ReCl}_3\text{-LiCl}$ (Re: La, Ce) Phase Diagrams, *J. Univ. Sci. Technol. Beijing.* 11 (1989) 598–603. <https://doi.org/10.13374/J.ISSN1001-053X.1989.06.034>.
- [31] X. Song, C. Zheng, An Investigation on the Phase Diagram of Ternary System $\text{LaCl}_3\text{-KCl-LiCl}$ (in Chinese), *Acta Chim. Sin.* 53 (1995) 978–984.
- [32] P. Bagri, M.F. Simpson, Determination of activity coefficient of lanthanum chloride in molten LiCl-KCl eutectic salt as a function of cesium chloride and lanthanum chloride concentrations using electromotive force measurements, *J. Nucl. Mater.* 482 (2016) 248–256. <https://doi.org/10.1016/j.jnucmat.2016.10.006>.
- [33] A. Samin, Z. Wang, E. Lahti, M. Simpson, J. Zhang, Estimation of key physical properties for LaCl_3 in molten eutectic LiCl-KCl by fitting cyclic voltammetry data to a BET-based electrode reaction kinetics model, *J. Nucl. Mater.* 475 (2016) 149–155. <https://doi.org/10.1016/J.JNUCMAT.2016.04.002>.
- [34] K. Nakamura, M. Kurata, *Materials Lanthanide Trichloride*, 247 (1997) 309–314.
- [35] R. Venkata Krishnan, K. Nagarajan, The pseudo-binary phase diagram of LiCl-KCl-LaCl_3 system, (2006). http://inis.iaea.org/Search/search.aspx?orig_q=RN:38095420 (accessed April 22, 2024).
- [36] S.L. Shang, Y. Wang, D.E. Kim, Z.K. Liu, First-principles thermodynamics from phonon and Debye model: Application to Ni and Ni_3Al , *Comput. Mater. Sci.* 47 (2010) 1040–1048. <https://doi.org/10.1016/j.commatsci.2009.12.006>.
- [37] Y. Wang, Z.K. Liu, L.Q. Chen, Thermodynamic properties of Al, Ni, NiAl , and Ni_3Al from first-principles calculations, *Acta Mater.* 52 (2004) 2665–2671. <https://doi.org/10.1016/j.actamat.2004.02.014>.
- [38] A. Van de Walle, G. Ceder, The effect of lattice vibrations on substitutional alloy thermodynamics, *Rev. Mod. Phys.* 74 (2002) 11–45. <https://doi.org/10.1103/RevModPhys.74.11>.

- [39] G. Kresse, J. Furthmuller, J. Furthmüller, J. Furthmuller, J. Furthmüller, J. Furthmueller, J. Furthmuller, J. Furthmüller, Efficient iterative schemes for ab initio total-energy calculations using a plane-wave basis set, *Phys. Rev. B-Condensed Matter*. 54 (1996) 11169–11186. <https://doi.org/10.1103/PhysRevB.54.11169>.
- [40] P.E. Blöchl, Projector augmented-wave method, *Phys. Rev. B*. 50 (1994) 17953–17979. <https://doi.org/10.1103/PhysRevB.50.17953>.
- [41] D. Joubert, From ultrasoft pseudopotentials to the projector augmented-wave method, *Phys. Rev. B - Condens. Matter Mater. Phys.* 59 (1999) 1758–1775. <https://doi.org/10.1103/PhysRevB.59.1758>.
- [42] J.P. Perdew, K. Burke, M. Ernzerhof, Generalized gradient approximation made simple, *Phys. Rev. Lett.* 77 (1996) 3865–3868. <https://doi.org/10.1103/PhysRevLett.77.3865>.
- [43] A. van de Walle, Multicomponent multisublattice alloys, nonconfigurational entropy and other additions to the Alloy Theoretic Automated Toolkit, *Calphad Comput. Coupling Phase Diagrams Thermochem.* 33 (2009) 266–278. <https://doi.org/10.1016/j.calphad.2008.12.005>.
- [44] M.W. Chase, J.L. Curnutt, J.R. Downey, R.A. Mcdonald, A.N. Syverud, E.A. Valenzuela, JANAF Thermochemical Tables, 1982 Supplement, *J. Phys. Chem. Ref. Data*. 11 (2009) 695. <https://doi.org/10.1063/1.555666>.
- [45] SGTE Substance Database - SGTE - Scientific Group Thermodata Europe, (n.d.). <https://www.sgte.net/en/neu>.
- [46] O. Redlich, A.T. Kister, Algebraic Representation of Thermodynamic Properties and the Classification of Solutions, *Ind. Eng. Chem.* 40 (1948) 345–348. <https://doi.org/10.1021/ie50458a036>.
- [47] A. Gelman, J.B. Carlin, H.S. Stern, D.B. Dunson, A. Vehtari, D.B. Rubin, *Bayesian Data Analysis*, Chapman and Hall/CRC, New York, 2013. <https://doi.org/10.1201/b16018>.
- [48] M.A. Newton, A.E. Raftery, Approximate Bayesian Inference with the Weighted Likelihood Bootstrap, *J. R. Stat. Soc. Ser. B*. 56 (1994) 3–48. <http://www.jstor.org/stable/2346025> (accessed September 24, 2023).
- [49] M.H. Norwood, C. V. Briscoe, Elastic Constants of Potassium Iodide and Potassium Chloride, *Phys. Rev.* 112 (1958) 45. <https://doi.org/10.1103/PhysRev.112.45>.
- [50] W. Zachariasen, *The UC13-type of Crystal Structure*, 1947. <https://books.google.com/books?hl=en&lr=&id=JN5euEip198C&oi=fnd&pg=PP3&dq=W.+H.+Zachariasen,+J.+Chem.+Phys.+16,+254+1948&ots=5JUWOCYgO3&sig=viArw6bUB5kU9eJGgwhKGP9A8so> (accessed May 1, 2024).